Angewandte Chemie
Eine Zeitschrift der Gesellschaft Deutscher Chemiker

Supporting Information

The Ti_3AlC_2 MAX Phase as an Efficient Catalyst for Oxidative Dehydrogenation of n-Butane

Wesley H. K. Ng, Edwin S. Gnanakumar, Erdni Batyrev, Sandeep K. Sharma, Pradeep K. Pujari, Heather F. Greer, Wuzong Zhou, Ridwan Sakidja, Gadi Rothenberg, Michel W. Barsoum, and N. Raveendran Shiju**

ange_201702196_sm_miscellaneous_information.pdf
ange_201702196_sm_Movie.wmv

Supporting Information

1. Experimental Section:

Ti_3AlC_2 MAX phase powder was obtained by reacting Ti_2AlC MAXthal (-325 mesh, Sandvik, Sweden) with TiC at 1350 °C for 2 h (heating rate was 10 °C/min). The -325 mesh, Ti_3SiC_2 powder was purchased from Sandvik, Sweden.

Powder X-ray diffractograms (XRD) were measured on a Miniflex II diffractometer using Cu Kα radiation operating at 30 kV and 15mA at an angle (2θ) range of 5-80°, with a step size of 0.02° and a speed of 1°/min.

The XPS measurements were performed at the Tata Steel IJmuiden. The as-received powder samples were first characterised using Kratos Ultra DLD XPS instrument. Each sample was placed in the quartz crucible prior to the XPS analysis and the sample surface was charge neutralized during the analysis by the charge compensation system of the XPS instrument. The XPS spectra were acquired with a hybrid mode (magnetic lens on). An Al-monochromated X-ray source was used at 15 mA and 15 kV to generate the X-ray photons and the emitted photoelectrons were collected from the area of 0.7 x 0.3 mm^2. The acquired XPS spectra were processed in CASA XPS software to quantify the obtained data and determine the presented surface compositions.

Transmission electron microscopic (TEM) images and selected area electron diffraction (SAED) patterns were attained using a JEOL JEM-2011 electron microscope fitted with a LaB_6 filament and operated at an accelerating voltage of 200 kV. The TEM images were recorded using a Gatan 794 multiscan CCD camera. HAADF STEM images, EDX spectra and elemental maps were collected on a FEI Titan Themis S/TEM fitted with an X-FEG gun and operated at 200 kV. Titan is equipped with a Super-X high sensitivity windowless EDX detector. HAADF STEM images were recorded using a FEI Ceta 16-megapixel CMOS camera.

n-Butane adsorption experiments were performed in a micro-calorimeter (Calvet C80, Setaram) at 523 K in isothermal condition, connected to a home built manometric apparatus. Blank experiment was carried out at 523 K by introducing a known amount of gas into the empty sample holder and measuring the equilibrium pressure. To calculate the amount of butane adsorbed, the blank curves are used with a correction for the volume occupied by the MAX phase sample itself. The sample is outgassed at 473 K for 6 hours before the adsorption measurements.

Procedure for catalytic activity tests:

The catalytic experiments were carried out in a parallel continuous six-flow reactor system, which is directly connected to a gas chromatograph (Interscience micro GC, with FID and TCD). Each reactor was loaded with 100 mg catalyst. The reaction temperature was varied from 500 °C to 650 °C. The total reaction feed of each reactor was 17 -50 ml/min, with a volumetric ratio of O_2:n-butane:argon varying from 0.25:1:18 to 1:1:18.

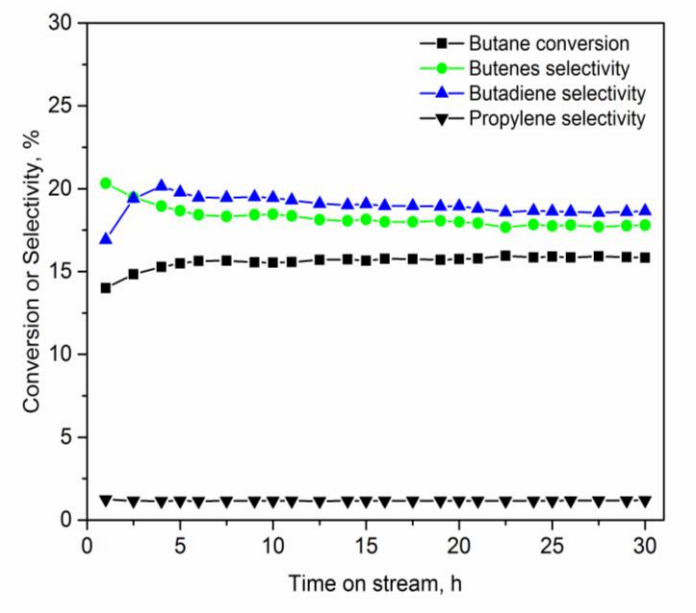

Figure S1. Stability test of Ti_3AlC_2. Reaction conditions O_2:C_4H_{10}:Ar = 1:1:18; 500 °C; flow rate 17 mL/min.

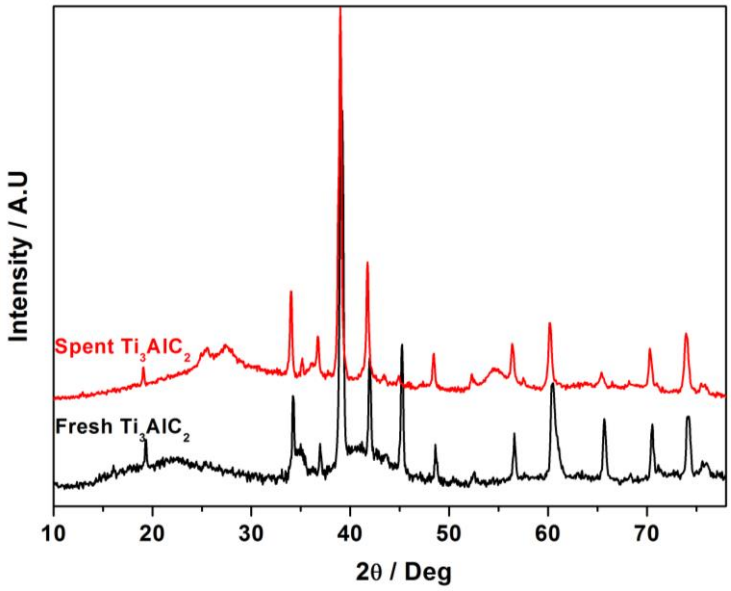

Figure S2. The X-ray diffraction patterns of fresh and used Ti_3AlC_2 MAX phase. The used (spent) sample is after a reaction of 30 hours.

2. PALS

Experimental procedure**:** PALS measurements were carried out using a fast-fast positron lifetime setup couple with two plastic scintillation detector placed opposite to each other. The time resolution of the spectrometer is 265 ps measured using ^{60}Co . A radioisotope (^{22}Na ~10 microcurie) enveloped between two kapton films (thickness ~8 micrometer) was used as positron source. The positron source

was immersed in adequate amount of TiC powder ensuring that all the emitted positrons annihilate within the powder sample. Silicon single crystal has been used as a reference material for the correction of positron annihilation from the source and kapton films. The PALS spectrum contained ~ 1×10^6 counts. PALS spectrum were analyzed into discrete positron lifetime components using PALSfit [J. V. Olsen, P. Kirkegaard, N. J. Pedersen and M. Eldrup, *Phys. Stat. Sol. C*, 2007, **4**, 4004-40006].

Table S1: Positron lifetime components and corresponding intensities in Ti_3AlC_2 sample.

Sample	**τ_1 (ps)**	**I_1(%)**	**τ_2 (ps)**	**I_2(%)**
Ti_3AlC_2	189.7±6.1	58.1±6.2	300.9±9.1	41.8±6.2

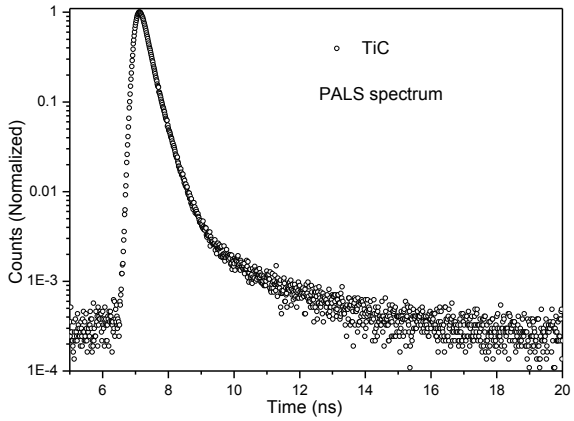

Figure S3: The PALS spectrum of Ti_3AlC_2 MAX phase sample.

3. TEM and EDX

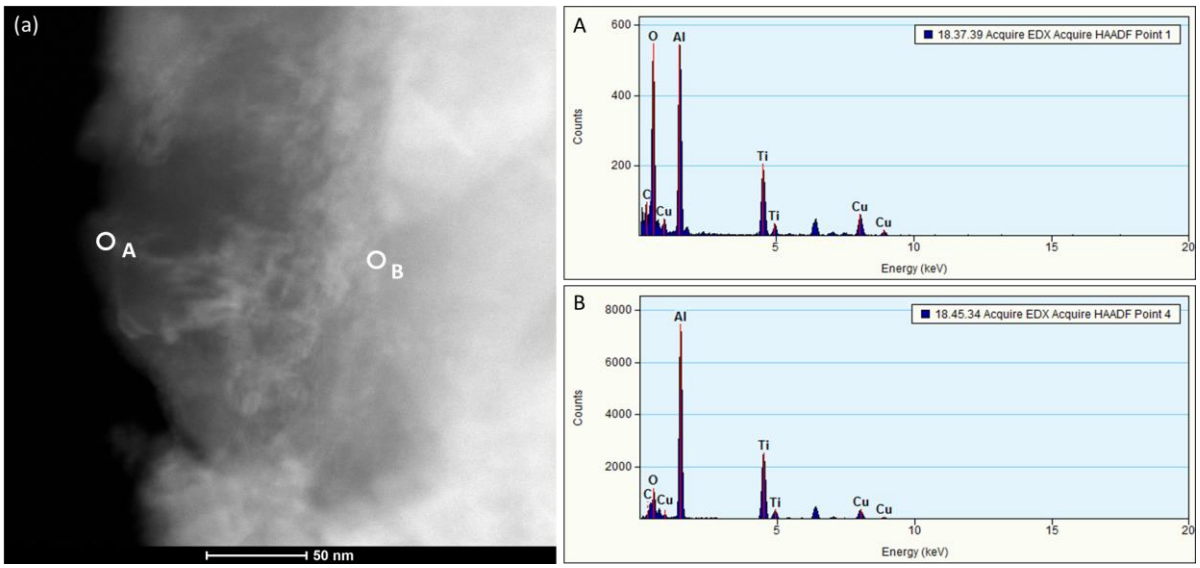

Figure S4. (a) HAADF STEM image of a Ti_3AlC_2 MAX phase containing an amorphous surface layer. A and B are EDX spectra recorded from the individual regions marked in the STEM image. Both EDX spectra show high quantities of Ti and Al with differing O Kα contents. Cu Kα and Kβ emission lines correspond to the TEM grid.

4. Catalytic activity of Ti_3SiC_2

Table S2. Performance of the Ti_3SiC_2 for butane ODH

Reaction Temperature, deg[a]	Butane conversion,%	Total selectivity of butenes,%	Selectivity of 1,3-BD,%[b]	Selectivity of prop,%[c]
450	3.8	1.6	1.9	0
500	5.1	2.6	3.8	0
550	10.2	2.3	4.5	0
600	15.5	2.3	4.4	1.0

[a]Reaction conditions: O_2:C_4H_{10}:Ar = 1:1:18; flow rate=17 mL/min; catalyst=0.1g; total pressure = 1bar. [b] BD=butadiene [c] prop=propylene; trace amounts of ethylene and methane were also produced; rest is carbon oxides.

5. Oxygen vacancy analysis

N_2O chemisorption is well known method to determine the exposed metal surface area of the transition metal catalysts since N_2O dissociation energy is significantly lowered only on metallic sites. We applied this method together with XPS analysis to find the MAX phase oxygen vacancies. For this, the sample was reduced in UHV (10^{-7} mbar) at 500 °C creating oxygen vacancies and subsequently exposed the reduced surface to N_2O. The optimisation experiments indicated that the surface re-oxidation with oxygen from N_2O occurs at 300 °C. We then examined the re-oxidised surface by XPS, which proved the surface Ti oxidation (see equation S1 below) and subsurface oxidation controlled by diffusion of O species (Figure S5). The XPS spectra in figure S6 show the reversible reduction and oxidation of the surface in our sample. We were able to repeat this reduction-oxidation cycle several times, showing the ability of the catalyst to undergo multiple redox cycles. The amount of Ti that undergoes oxidation can be estimated by linear extrapolation of the subsurface (diffusion dependent oxidation) uptake to t=0 (see Figure S5), which gives 3.5 at%. According to the dissociative reaction $2N_2O$ (gas) + $Ti^0_s \rightarrow (TiO_2)_s + 2N_2$ (gas), the corresponding oxygen amount will be 7.0 at%. This is the amount of oxygen atoms in the XPS measuring slot of 0.21 mm^2 and 8 nm of XPS probing depth. Considering Ti_3AlC_2 density of 4150 kg/m^3 and the molecular weight of 194.6, the concentration of oxygen vacancies can be estimated as $9\times 10^{26}/m^3$.

$$2N_2O\ (gas) + Ti^0_s \rightarrow (TiO_2)_s + 2N_2\ (gas) \qquad [S1]$$

The oxidised surface was examined by XPS.

Experimental

XPS spectra were obtained using a Kratos Axis Ultra DLD XPS instrument. A monochromatic Al K_α X-ray source was used for all samples, along with base pressure in the analysis chamber of 10^{-9} mbar. The samples were placed in the quartz crucible in order to use them in the reaction cell; therefore the charge neutralizer was used during all XPS measurements. The conditions used for all of the survey scans were as follows: energy range 0 - 1200 eV, pass energy of 160 eV, step size of 1.0 eV, sweep time of 180 s and X-ray spot size was chosen in a slot mode of 700 x 300 μm^2. The high-resolution

spectra were acquired within an energy range of 40–20 eV, depending on the peak being examined, with a pass energy of 20 eV and a step size of 0.1 eV.

The procedure of the experiments was as follows: first, the MAX phase powder was placed in a quartz crucible and XPS spectra were obtained of initial as received surface. Subsequently the sample was reduced in UHV of 10^{-7} mbar in a reaction chamber for 1 hour at 500 °C. The sample was then transferred to an analysis chamber without breaking UHV where XPS spectrum of reduced state was recorded. Subsequently the powder was placed back to the reaction chamber again without breaking the vacuum. The sample was then exposed to 100 % N_2O gas flow for 1 min at 300 °C. The chamber was pumped back to vacuum directly after the N_2O exposure and cooled down to 100 °C prior to the transfer for XPS analysis.

Sample preparation

The MAX phase powder sample in as-received state was inserted to the UHV setup for XPS analysis. The reduction in UHV of 10^{-7} mbar at 500 °C and chemisorption in 1 bar N_2O (5N purity) were performed in the reaction cell that is directly attached to the XPS setup. This setup allows us to pump the reaction gases after each treatment, down to UHV, and directly transfer the reacted surfaces to analysis chamber for XPS analysis avoiding any contact with air. Thus, the reacted sample surface was subsequently examined by XPS after each treatment step in the reaction cell.

Prior to the experiments, the empty quartz crucible was heated in a vacuum to 1000°C to remove any adsorbed H_2O.

XPS spectral analysis

The XPS spectra were processed using Casa XPS software. The binding energy was calibrated using the adventitious C 1s peak to a fixed value of 284.8 eV or carbide peak at 281.3 eV. After calibration, the background from each spectrum was subtracted using a Shirley background to remove most of the extrinsic loss structure. All survey scans were analysed to determine the stoichiometry of the compound by using the appropriate sensitivity factors and to determine the amount of adventitious carbon and contaminants present.

Results

There is a clear surface oxidation according to the reaction [S1] and subsurface oxidation controlled by diffusion of O species (Figure S5).

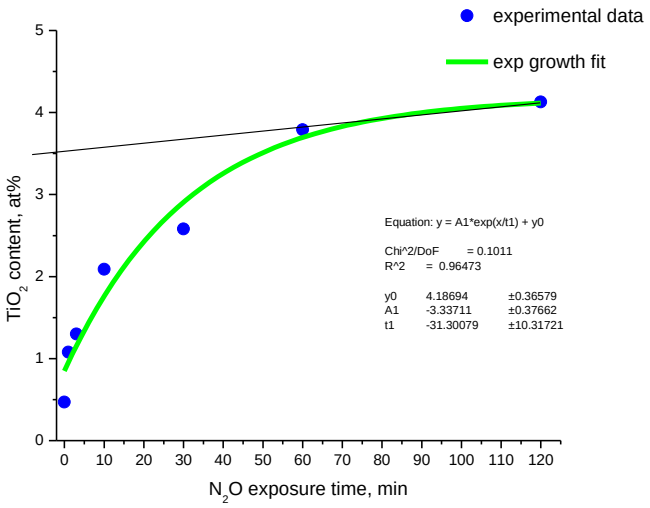

Figure S5. Oxygen uptake by Ti from MAX phase obtained by the XPS analysis of the sample exposed to N_2O at 300 °C. Blue dots are experimental data while green line is exponential fitting (formula is shown in the figure).

The quantified Ti contribution of 3.5 at% (Figure S5) by extrapolation of subsurface contribution to t=0 according to reaction [S1] will take 2 x 3.5 at% = 7.0 at% of oxygen atoms. This is the amount of the outermost surface oxygen vacancies calculated from the intersection of the surface and subsurface (diffusion dependent oxidation) uptakes (Figure S5). The obtained amount of oxygen atoms was detected within the XPS measuring volume of 0.21 mm^2 x 8 nm (probing depth). Considering Ti_3AlC_2 density of 4150 kg/m^3 and its molecular weight of 194.6, the concentration of oxygen vacancies is 9 $x10^{26}$ per m^3. The XPS spectra (Figure S6) are also shown below to demonstrate the surface and subsurface oxidation of Ti.

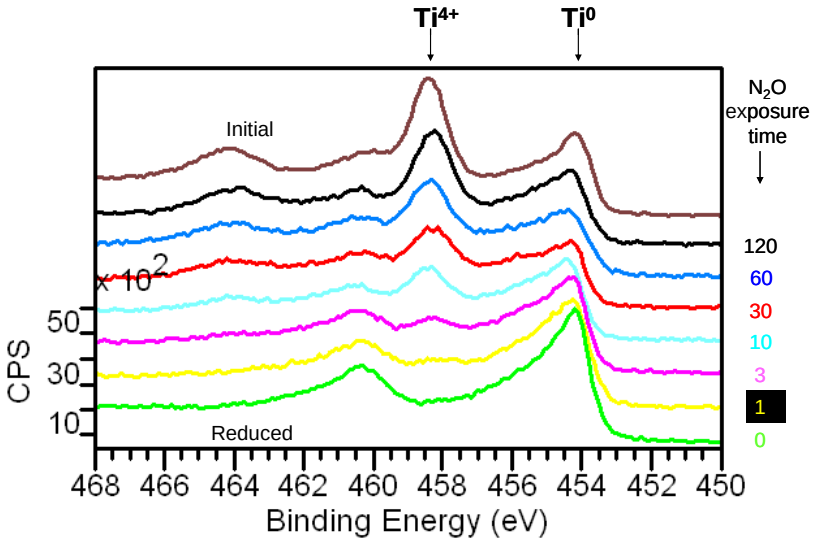

Figure S6: Ti 2p XPS spectra of MAX phase samples upon reduction in UHV of 10^{-7} mbar at 500 °C and subsequent N_2O exposure at 300 °C. The initial as-received sample (top spectrum) is added for a comparison.

Calculation of oxygen vacancies in Ti_3AlC_2 MAX phase by XPS combined with N_2O chemisorption

Probing volume by XPS:

Height = 7.6×10^{-9} m; Area = 2.1×10^{-7} m^2

$\therefore$ Volume = 1.6×10^{-15} m^3 = 1.6×10^{-9} cm^3

Corresponding weight of the catalyst = (1.6×10^{-9} cm^3) $\times$ (4.15 g/cm^3) = 6.64×10^{-9} g

(4.15 g/cm^3 is the density of Ti_3AlC_2)

Corresponding number of moles = 6.64×10^{-9} / 194.6 (Mol. wt. of Ti_3AlC_2 is 194.6)

= 3.41×10^{-11}

Corresponding number of atoms = (3.41×10^{-11}) (6.022×10^{23}) = 2.05×10^{13}

Corresponding number of oxygen vacancies = $(2.05 \times 10^{13} \times 7) / 100$

(7% from XPS+N_2O analysis) = 1.435×10^{12}

$\therefore$ No. of oxygen vacancies in 1 cm^3 of Ti_3AlC_2 = $1.435 \times 10^{12} / 1.6 \times 10^{-9}$ = 8.97×10^{20}

No. of oxygen vacancies in 1 m^3 of Ti_3AlC_2 = 8.97×10^{26}

No. of oxygen vacancies per 1 g of catalyst = 2.16×10^{20}

(density of Ti_3AlC_2 = 4.15 g/cm^3)

6. Adsorption isotherms

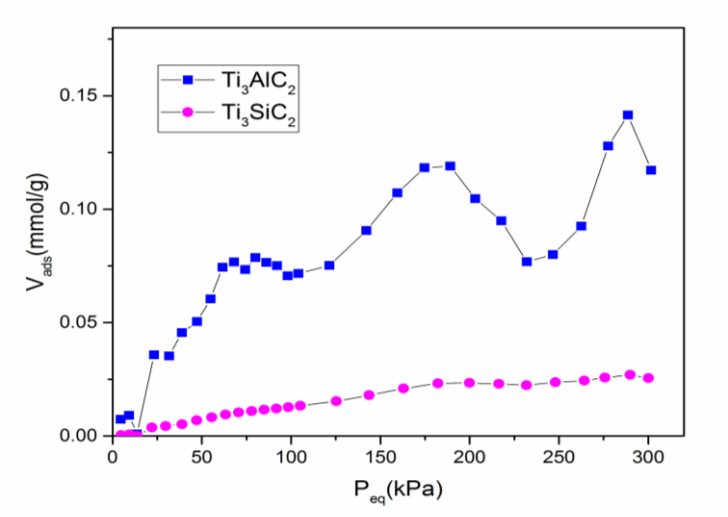

Figure S7. The adsorption isotherms of n-butane on Ti_3AlC_2 and Ti_3SiC_2 at 250 °C show that the composition of MAX phase has a significant influence on the adsorption properties.

7. Modelling studies

We noticed from the previous equilibrium study on the Ti-Al-O ternary system[1] that, there exists a stable ternary phase of Al_2TiO_5[2]. For simplicity, we used the O-terminating (001) surface of the ternary phase as a simple model to represent a mixed-cation oxide surface of the MAX at a relatively lower temperature. At higher temperatures (> 1100°C), the surface of the oxidized MAX phase is typically dominated by the α-Al_2O_3 phase[3]. But, such a high temperature was not part of our catalytic studies.

We have performed the electronic structure calculations as implemented in the Density Functional Theory approximation as implemented in VASP ab-initio code[4] to assess on the energetics on the adsorption of butane onto the oxygen-terminating surface at the ground state (0K). While further details of the methodology, exchange-correlation potentials used (PAW-PBE[5]) and convergence criteria (electronic convergence criterion of 10^{-5} eV and force convergence limit of 10^{-2} eV/A°) have been given elsewhere[6], we would like to emphasize here the high energy cut-off level that we employed (500 eV) to ensure the high precision of the cohesive energy calculations. Table S3 shows the list of chemical reactions along with the pictures of the final atomic configurations.

First butane is adsorbed on the surface of Al_2TiO_5 through the formation of the C-O bond on the surface, followed immediately by the dissociation of the hydrogen atom onto the surface, captured by one of the oxygen's dangling bond (we supplemented a video to show the relaxation sequence):

$$C_4H_{10(g)} + O_{(surface)} \rightarrow C_4H_{9(ads)} + OH_{(ads)} \qquad \Delta H = -2.99 \text{ eV (intermediate reaction \# 1)}$$

We found that there is a slightly favorable energy for a possible subsequent reaction whereby the adsorbed C_4H_9 further decomposes into $C_4H_{8(ads)}$ by releasing another hydrogen atom forming a water molecule:

$$C_4H_{9(ads)} + OH_{(ads)} \rightarrow C_4H_{8(ads)} + H_2O_{(ads)} \qquad \Delta H = -0.36 \text{ eV (intermediate reaction \# 3)}$$

which gives an overall chemical reaction of:

$$C_4H_{10(g)} + O_{(surface)} \rightarrow C_4H_{8(ads)} + H_2O_{(ads)} \qquad \Delta H = -3.35 \text{ eV (overall reaction no 4)}$$

A further oxidative dehydrogenation may be facilitated by the release of more hydrogen atoms from the adsorbed C_4H_8 yielding 1,3 butadiene

$$C_4H_{8(ads)} + O_{(ads)} \rightarrow C_4H_{6(ads)} + H_2O_{(ads)} \qquad \Delta H = -1.39 \text{ eV (intermediate reaction no 4)}$$

Overall, we found that releasing two or four hydrogen atoms from butane onto the surface yielding adsorbed water molecule/OH bonds formation results in very favorable chemical reactions:

$$C_4H_{10(g)} + O_{(surface)} \rightarrow C_4H_{8(g)} + H_2O_{(ads)} \qquad \Delta H = -2.50 \text{ eV (overall reaction no 3)}$$

$$C_4H_{10(g)} + 4O_{(surface)} \rightarrow C_4H_{6(g)} + 4OH_{(ads)} \qquad \Delta H = -4.77 \text{ eV (overall reaction no 8)}$$

We do notice however that the dissociation of the adsorbed $C_4H_{8(ads)}$ from the surface (combining the intermediate reaction # 4 and 5 from the intermediate as listed in Table S3) is an endothermic reaction: $C_4H_{8(ads)} \rightarrow C_4H_{8(g)}$ $\Delta H = 0.85$ eV. While this value is certainly much less than the energy required to release the intermediate product of $C_4H_{9(ads)}$ into $C_4H_{9\,(g)}$ i.e. the intermediate reaction # 2 with $\Delta H = +3.89$ eV, such a direct dissociation may not necessarily be the easiest pathway and other

mechanisms may possibly take place to lower these energy barriers. This points to the possible role of a higher operating temperature to enable the reaction to proceed. Nevertheless, the overall reactions do indicate the energetically favorable conditions for oxidative dehydrogenation of butane.

Table S3

REACTION #	BUTANE	SUBSTRATE	BUTANE+ SUBSTRATE	INTERMEDIATE C_4H_9(ads) + H(ads)	FINAL PRODUCTS	ΔH (FROM INTERMEDIATE)	ΔH (OVERALL)
1	-73.5603	-518.8674	-592.4277	-595.4219	C_4H_9(ads) + H(ads)		-2.9942
2					C_4H_9(g) + H(ads)		
	-73.5603	-518.8674	-592.4277	-595.4219	-591.5307	3.8912	0.8970
3					1-Butene(g) + 1 WATER(ads)		
	-73.5603	-518.8674	-592.4277	-595.4219	-594.9265	0.4953	-2.4988
4					1-Butene(ads) + 1 WATER(ads)		
	-73.5603	-518.8674	-592.4277	-595.4219	-595.7813	-0.3595	-3.3536
5					1-Butene(g) + 2OH(ads)		
	-73.5603	-518.8674	-592.4277	-595.4219	-593.4835	1.9383	-1.0558
6					1-Butene(ads)+ 2OH(ads)		
	-73.5603	-518.8674	-592.4277	-595.4219	-596.8012	-1.3793	-4.3735
7					1,3 Butadiene(g) + 2 WATER		
	-73.5603	-518.8674	-592.4277	-595.4219	-594.5075	0.9144	-2.0797
8					1,3 Butadiene(g) + 4OH (ads)		
	-73.5603	-518.8674	-592.4277	-595.4219	-597.2005	-1.7786	-4.7727

FIGURES: REACTION PRODUCTS FROM 1-8

(Ti is represented by blue balls and O by red balls)

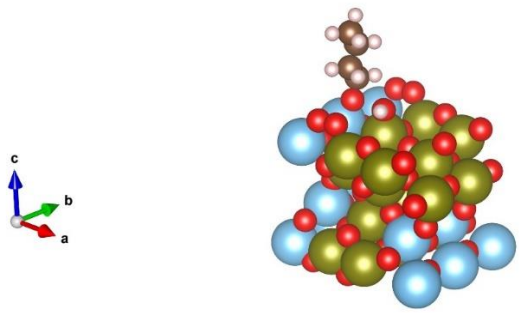

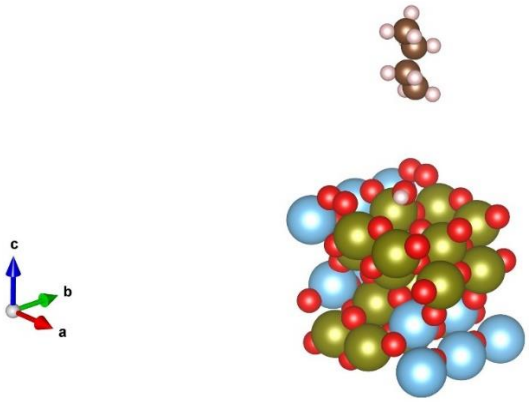
c
b
a

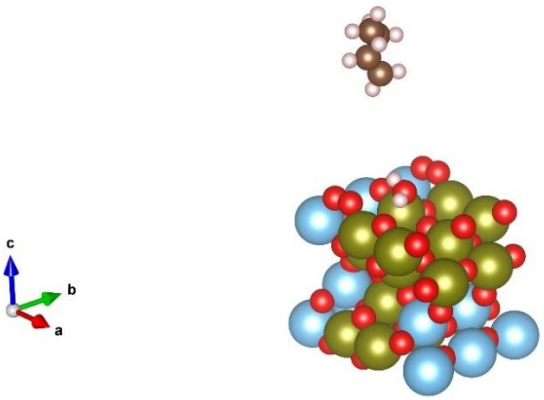
c
b
a

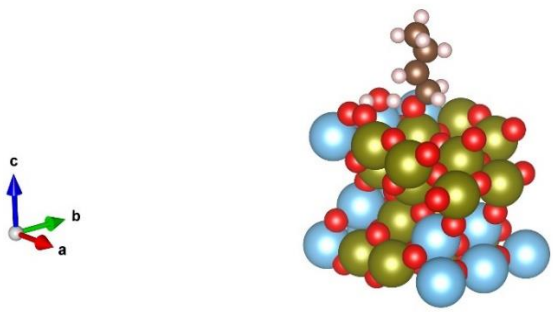
c
b
a

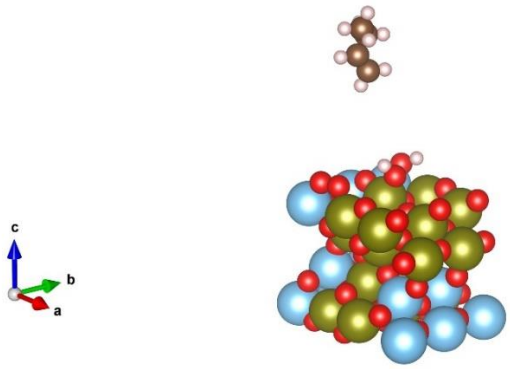
c
b
a

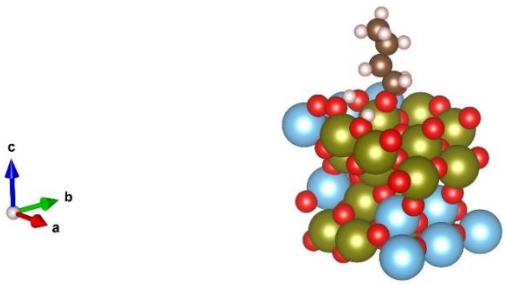
c
b
a

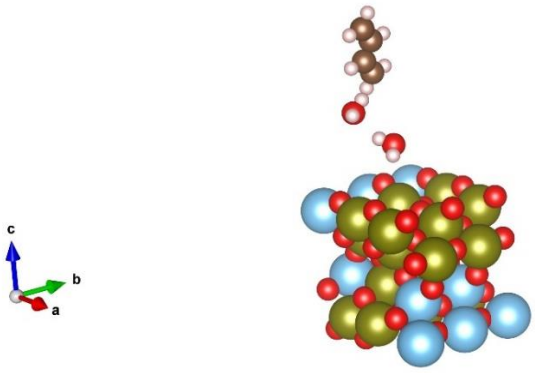
c
b
a

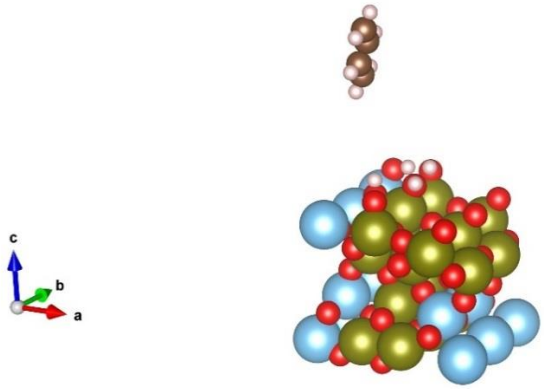

References:

1. Das, S., The Al-O-Ti (Aluminum-oxygen-titanium) system. *J. Phase. Equ.* **23**, 525-536 (2002).
2. Morosin, B.; Lynch, R. W., Structure studies on Al_2TiO_5 at room temperature and at 600°C. *Acta Crystallogr., Sect. B: Struct. Sci.* **28**, 1040-1046 (1972).
3. (a) Smialek, J. L.; Harder, B. J.; Garg, A., Oxidative durability of TBCs on Ti_2AlC MAX phase substrates. *Surf. Coat. Technol.* **285**, 77-86 (2016); (b) Wang, X. H.; Zhou, Y. C., Oxidation behavior of Ti_3AlC_2 at 1000–1400 °C in air. *Corros. Sci.* **45**, 891-907 (2003).
4. Kresse, G.; Furthmüller, J., Efficient iterative schemes for *ab initio* total-energy calculations using a plane-wave basis set. *Phys. Rev. B.* **54** , 11169-11186 (1996).
5. Perdew, J. P.; Burke, K.; Ernzerhof, M., Generalized Gradient Approximation Made Simple. *Phys. Rev. Lett.* **77***,* 3865-3868 (1996).
6. (a) Li, N.; Sakidja, R.; Ching, W.-Y., Ab initio study on the adsorption mechanism of oxygen on Cr_2AlC (0 0 0 1) surface. *Appl. Surf. Sci.* **315**, 45-54 (2014); (b) Li, N.; Sakidja, R.; Ching, W.-Y., Oxidation of Cr_2AlC (0001): Insights from Ab Initio Calculations. *JOM* **65***,* 1487-1491 (2013).